

# Impact Behavior and Energy Transfer Efficiency of Pulse-Driven Bent-Beam Electrothermal Actuators

Yoshinobu Shimamura, Kabir Udeshi, Long Que, *Member, IEEE*, Jaehyun Park, and Yogesh B. Gianchandani, *Senior Member, IEEE*

**Abstract**—This paper investigates the dynamics of bent-beam electrothermal actuators and their use in impact actuation of other micromechanical elements, and in particular the issue of energy efficiency achieved by temporal variations in electrical drive signals. A transient thermal model of an actuator beam shows that the uniformity of temperature profile is greater when activating with short electrical pulses, which results in larger achievable displacements and forces. A dynamic force analysis reveals that using a train of pulses, referred to as a burst pulse, for activation achieves significant impact forces due to high velocities at the point of impact. The analytical trends are confirmed through experimental observations of microfabricated metal test structures in which actuators work against bistable mechanisms. Measurements of 2 mm and 3mm long actuators show that pulsed activation results in  $> 5\times$  reduction in energy consumption, with the activation energy falling from over 1000  $\mu\text{J}$  at dc activation, to less than 200  $\mu\text{J}$  using a 0.2-ms voltage pulse. The actuators however consume higher instantaneous power levels at shorter pulses, which may inhibit the use of pulses less than 1 ms in width. Further, the energy consumption through burst activation is 70% that of a single pulse, if sufficient impact forces are generated. [1566]

**Index Terms**—Bent-beam electrothermal actuator, bistable structure, burst pulse drive, single pulse drive.

## I. INTRODUCTION

ELECTROTHERMAL actuators have proven to be effective in a number of applications and are favored for their ability to generate forces in the milli-Newton range, while being comprised of relatively simple structures occupying a small footprint. A measure of their versatility may be obtained through the wide spectrum of devices in which they have been employed. They have been used to construct linear and rotary motors [1], [2], variable optical attenuators [3], [4], fully mechanical oscillators [5], high-voltage generators [6], radio frequency switches [7], [8] and tactile displays [9]. The actuators are typically implemented in two configurations:

Manuscript received April 4, 2005; revised July 6, 2005. This effort was supported in part by a Career award from the U.S. National Science Foundation to Y. B. Gianchandani, and an award from the Ministry of Education, Culture, Sports, Science and Technology, Japan to Y. Shimamura. The research was carried out in the Michigan Nanofabrication Facility at the University of Michigan, Ann Arbor. Subject Editor C.-J. Kim.

Y. Shimamura was with the University of Michigan, Ann Arbor, MI 48109 USA. He is now with the Shizuoka University, Hamamatsu, Shizuoka 432-8561, Japan (e-mail: tysimam@ipc.shizuoka.ac.jp).

K. Udeshi, J. Park, and Y.B. Gianchandani are with the College of Engineering, University of Michigan, Ann Arbor, MI 48109 USA (e-mail: kudeshi@umich.edu, jaehyunz@umich.edu, yogesh@umich.edu)

L. Que was with the University of Michigan, Ann Arbor, MI 48109 USA. He is now at GE Global Research, Niskayuna, NY 12309 USA (e-mail: que@research.ge.com).

Digital Object Identifier 10.1109/JMEMS.2005.863696

bent-beam and pseudo-bimorph. Pseudobimorph actuators use the difference in the thermal expansion of two joined beams to generate displacement along an arc by Joule heating, and are inspired by conventional thermostats. On the other hand, a bent-beam actuator, constructed of a single conductive material, consists of a V-shaped beam that generates linear motion due to the outward expansion of its apex. Electrothermal actuators are capable of generating tens of microns of displacement.

Since reported by Que *et al.* [10], [11], a significant amount of effort has been invested in understanding the physics of operation of bent-beam actuators. An accurate model is desirable in order to optimize the performance of these actuators and push the limits of operation. Lott *et al.* [12] developed a steady-state model, which was improved upon by Giesberger *et al.* [13]. These models were expanded to include the transient response of actuators. The transient characteristics indicated that, instead of using a dc voltage, superior performance might be obtained through the use of a pulsed voltage supply. In addition to insights gained through modeling, experiments carried out by Que *et al.* [14] showed that the lifetime of actuators might be substantially improved by pulsed activation.

Actuators are generally used to overcome an opposing force, which may be in the form of a compliant spring, air damping, etc., or more often than not, a combination of these effects. In order to employ these actuators, a designer would like to use a minimum amount of energy to overcome this opposing force. Energy conservation is especially important for electrothermal actuators as they dissipate Joule heat, imposing challenging demands on electrical power sources. The analysis and experiments conducted explore methods to improve the energy efficiency of these actuators by a suitable pulsed activation method. In particular, the effort described in this paper addresses the power and energy necessary to switch a bistable mechanism. Such mechanisms [15]–[17] have been used with electrothermal actuators to maintain a displacement or force, even after the actuator power is turned off. Applications include, for example, RF and optical fiber switches. Further, the dynamics of actuators have been analyzed to understand the characteristics of the generated forces, and the influence of impact. Experiments carried out validate trends indicated through theoretical studies.

For an electrothermal actuator, an increase in the displacement under a zero force condition implies an increase in the maximum force that can be generated for a given displacement as seen from a typical force-displacement curve in Fig. 1[11]. Throughout this paper the maximum force and displacement attainable by a given actuator are used as complimentary performance metrics.

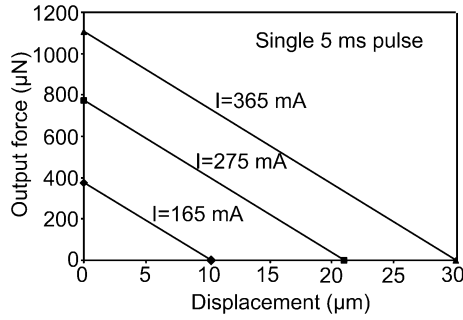


Fig. 1. Typical force displacement curve for a bent-beam electrothermal actuator. An increase in the maximum displacement implies an increase in the maximum output force generated.

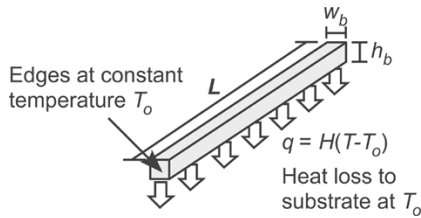


Fig. 2. Model to determine the temperature profile  $T(x, t)$  along the length of an electrothermal actuator.

Section II describes the thermal model developed for the actuator beam and its use to determine the energy efficiency and velocity of bent-beam actuators under various driving conditions. Section III explains the use of the bistable mechanism to impose a calibrated loading force, and an analysis of the velocity required to generate an appreciable impact force, in relation to the mass of the actuator. This analysis guides the design of a test structure consisting of the bistable mechanism, which is described. The fabrication process is described in Sections IV. Sections V and VI, respectively, present simulations and experimental results that validate analytical trends obtained and Section VII end with concluding remarks.

## II. ANALYSIS OF PULSED ACTUATION

In order to develop an intuitive understanding of the benefits of pulsed actuation, we develop a simplified thermal model of a bent-beam actuator, shown in Fig. 2. The actuator is constructed as a floating, V-shaped beam, clamped at its two ends to anchors, with Joule heat generated along the length of the beam. The constitutive equation for the temperature  $T$ , changing with distance  $x$ , along the length of the beam, and time  $t$ , is [18]

$$\frac{\partial T}{\partial t} = \alpha \frac{\partial^2 T}{\partial x^2} + \frac{q}{\rho \cdot c_p} - \frac{H(T - T_0)}{\rho \cdot c_p \cdot h_b} \quad (1)$$

where,  $\alpha$  is the thermal diffusivity,  $w_b$  and  $h_b$  are the width and height of the beam respectively,  $\rho$  the density,  $c_p$  the specific heat capacity,  $H$  is the heat transfer coefficient from the beam to the substrate, which is at a fixed temperature  $T_0$ , and  $q$  is the heat generated per unit volume of the beam. The anchors and substrate are assumed to be at a constant ambient temperature  $T_0$ .

In obtaining a solution to the model developed, constant values are assumed for  $c_p$ ,  $H$ ,  $\alpha$ , and  $q$  at all locations along

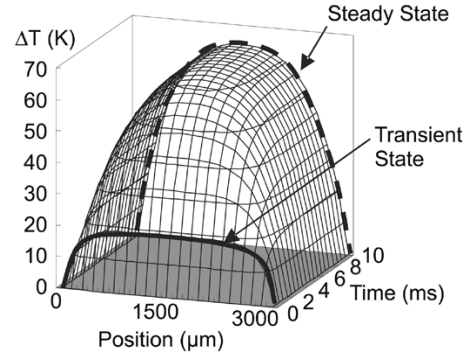


Fig. 3. Temperature profile along the length of the beam changing with time. The temperature during the transient state is fairly uniform at all positions along the beam. However as time progresses, the profile becomes elliptical, as indicated at a time of 10 ms, which can be regarded as steady state.

TABLE I  
PARAMETERS USED FOR DETERMINING THE TEMPERATURE PROFILE ALONG THE ACTUATOR BEAM USING THE FINITE DIFFERENCE METHOD. THE VALUES USED ARE TYPICAL FOR ELECTROPLATED COPPER

Parameter	Symbol	Value	Units
Thermal diffusivity	$\alpha$	$1.14 \times 10^8$	$\mu\text{m}^2/\text{s}$
Specific heat	$c_p$	$3.86 \times 10^{14}$	$\text{pJ}/\text{kg}/\text{K}$
Density	$\rho$	$8.90 \times 10^{-15}$	$\text{Kg}/\mu\text{m}^3$
Joule heat	$q$	$2.70 \times 10^6$	$\text{pW}/\mu\text{m}^3$
Heat transfer coefficient	$H$	$6.00 \times 10^4$	$\text{pW}/\mu\text{m}/\text{K}$
Width	$w_b$	10	$\mu\text{m}$
Height	$h_b$	27	$\mu\text{m}$
Length	$L$	3000	$\mu\text{m}$
Maximum time		10	ms
Length segments		30	
Time interval		500	
Position increment		100	$\mu\text{m}$
Time increment		$2.00 \times 10^{-5}$	s
Convergence parameter		0.229	

the length of the beam. Also, heat loss from the sides and top of the actuator beam is neglected. (A shape factor could be introduced to account for the additional heat loss [19].) Although these assumptions can lead to errors while developing an accurate model [12], [13], they help facilitate a working solution that yields a qualitative understanding of pulsed actuation. The model is solved using the finite difference method (explicit form), to obtain the temperature profile along the beam changing with time, shown in Fig. 3. The parameters used for the analysis are shown in Table I, and are typical values for electroplated copper.

We observe that in the transient state, the temperature profile along the length of the beam is relatively uniform. This is in stark contrast to the elliptical temperature profile generated at steady state (10 ms). A flat temperature profile is desired, as a given actuator, for the same peak temperature of the beam, generates a larger displacement. This may be illustrated as in Fig. 4, which shows the temperature profile when an actuator beam is heated at power levels of 286 mW for 10 ms and 561 mW for 1 ms. The peak change in temperature reached, using

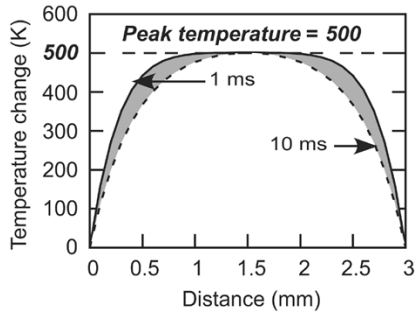


Fig. 4. The peak temperature change of the actuator beam is 500 K, when driven with pulse widths of 1 ms and 10 ms at different power levels. The difference in the area under the curve (shaded area) for the two activation pulse widths indicates the displacement generated will be different.

either actuation method, is 500 K. If this is the maximum temperature change allowed by material constraints, then neither actuation method will damage the beam. However, the maximum displacements generated are different, being determined by the area under the curves. This may be further elucidated by the expression for the change in length  $\Delta L$  of the bent-beam actuator

$$\Delta L = \alpha_L L \int_0^L (T(x) - T_o) dx \quad (2)$$

where  $\alpha_L$  is the coefficient of linear expansion and  $L$  the length of the beam. The increase in length, which determines the displacement of the actuator, depends on the integral term. The integral term is the area under the curve in Fig. 4.

Since the area under the curve is greater using a 1 ms pulse, pulsed activation of bent-beam actuators gives the potential to generate larger displacements, which implies larger forces, with a given actuator. The results of this analysis are validated through experimental observations in Section VI.

A reduction in the pulse width achieves an increase in the maximum displacement attainable with a given actuator, while requiring a higher amount of instantaneous power. In an effort to use the advantages of moving to shorter pulse widths ( $< 1$  ms), without using an excessively high instantaneous power level, the use of a burst pulse, which is a series of short pulses [see Fig. 5(a)], is investigated. Burst pulse activation results in a high actuator velocity at the point of contact, determined using the temperature profile obtained using the finite difference method. Equation (2) is used to estimate the change in length of the actuator, hence its displacement and velocity. While using a single pulse actuation method, the velocity of the actuator starts at its maximum and then exponentially decays, so that at the time of contact ( $> 1$  ms) it has fairly small value [see Fig. 5(b)]. However the use of a burst pulse results in high velocity oscillations, due to the alternating effects of Joule heating and thermal dissipation. It will be shown through a force analysis (see Section III) that this higher velocity achieved has significant implications on energy consumption because of the impact force that it provides.

### III. BISTABLE MECHANISM AND ROLE OF ACTUATION VELOCITY

The pulsed and burst activation methods were compared by imposing a minimum loading force requirement through the use

of a compliant bistable mechanism [15]–[17]. These mechanisms have two states or modes of operation, which can be referred to as the “initial” mode and the “snapped” mode, and can be discerned from their force-displacement characteristics shown in Fig. 6(a). When an increasing force is applied to a bistable mechanism in the initial mode, a modest increase in displacement is observed up to the upper bifurcation point. At the upper bifurcation point, a sudden large displacement is observed without the application of any additional force. This large displacement results in the structure being driven into its snapped mode, and remains in this mode, without the application of an additional force. A similar large decrease in displacement is observed at the lower bifurcation point, when the applied force is in the reverse direction. The mechanism returns to its initial mode from the snapped mode. By scaling its various dimensions, the bifurcation points of the bistable structure can be tuned.

An alternative method to analyze a bistable mechanism is through its potential energy curve [see Fig. 6(b)]. It shows that the structure has two energy valleys, which correspond to two stable positions in the two modes of operation. The two valleys are unequal, and the reaction force of the bistable structure is highly nonlinear with displacement.

The test structure is constructed using a bistable mechanism, sandwiched between bent-beam actuators on either side [see Fig. 7(a)]. The actuators are used alternately to switch the bistable mechanism between its two modes. Actuator A is used to switch the bistable mechanism from initial to snapped mode and actuator B is used to go from the snapped mode back to initial mode. A change in mode is observed as a structural change through the microscope.

The bistable mechanism [see Fig. 7(b)] is derived from its counterpart constructed using springs and pin joints, shown in Fig. 7(c). In order to microfabricate the mechanism, it is redesigned using compliant members. Every element of the bistable mechanism is important to get well-defined potential valleys, shown in Fig. 6. The slender beams,  $Lb_1$  and  $Lb_3$ , primarily serve as pin joints, where as the spring is included using the beam  $Lb_5$ . The thick beam,  $Lb_2$ , provides the required stiffness.

The force that must be applied on the bistable mechanism to switch it between its two modes, using either actuator A or B, is used as a reference to compare various driving conditions for a single actuator. For example, Actuator A must drive the mechanism through a distance  $\delta_{\text{switch}}$  [see Fig. 6(b)], while overcoming a peak force corresponding to the upper bifurcation point, in order to go from the initial mode to the snapped mode.

#### A. Force Analysis

The bent-beam actuator makes contact with the bistable mechanism while traveling at a nonzero velocity. This velocity results in an impact force and an analysis is carried out to investigate the effect of the generated impact force. The following analysis may be extended to any situation in which an actuator, used to generate force, contacts the actuated element with a finite velocity.

Both the bent-beam actuator and the bistable mechanism are modeled as equivalent lumped elements shown in Fig. 8.  $m_1$  is an equivalent mass of the electrothermal actuator,  $m_2$  is an

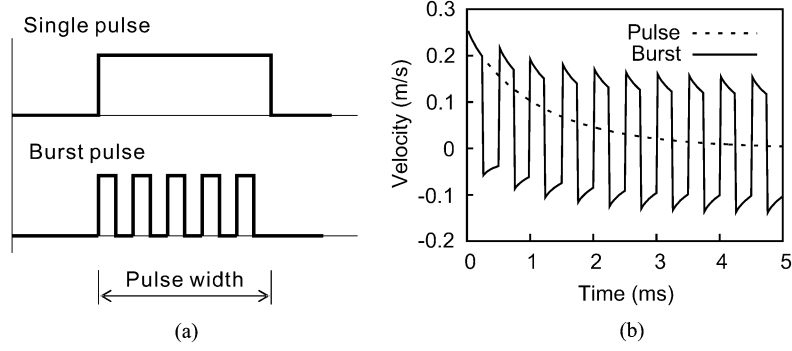


Fig. 5. (a) Schematic showing single pulse and a burst pulse. (b) The velocity of a bent-beam actuator being activated with a single pulse and a burst pulse at the same power level, evaluated using the finite difference method.

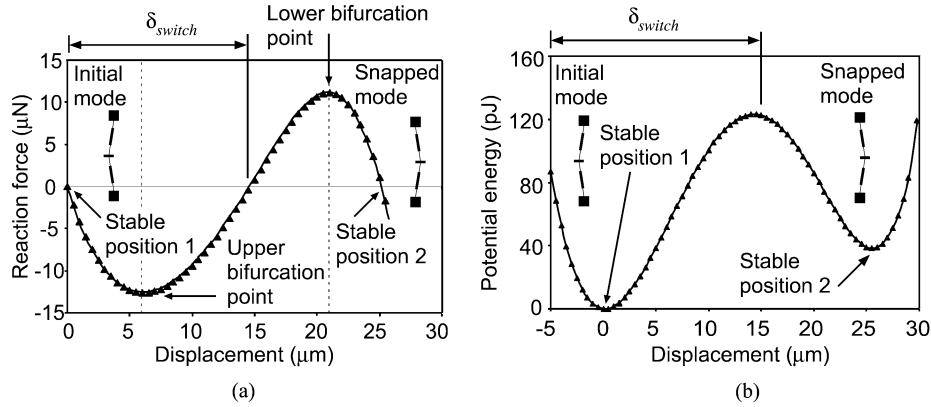


Fig. 6. (a) Force-displacement characteristics of a bistable mechanism showing the upper and lower bifurcation points (b) Potential energy curve of the bistable mechanism with the two energy valleys being the stable positions of the mechanism. The minimum displacement required to cause a change in mode of the mechanism is referred to as  $\delta_{switch}$ , as shown.

equivalent mass of the bistable mechanism and  $k_2$  is an equivalent linear spring of the bistable mechanism. The equivalent mass,  $m_{eq}$ , of the actuator or bistable mechanism can be determined by considering them as springs of mass  $m_s$  [20].

$$m_{eq} = \frac{1}{3}m_s. \quad (3)$$

The stiffness of spring  $k_2$  is assumed to be linear within the region of interest. From the principle of conservation of momentum, the momentum of the system before and after the impact are equated

$$m_1(v_1 - v'_1) = m_2v_2 \quad (4)$$

where  $v_1$  is the velocity of  $m_1$  before impact,  $v'_1$  is the velocity of  $m_1$  after impact and  $v_2$  is the velocity of  $m_2$  after impact. If an impact force is generated,  $v_2$  should be larger than or equal to  $v'_1$ , then

$$\begin{aligned} v_2 &= \frac{m_1}{m_2}(v_1 - v'_1) \geq v'_1 \\ \therefore v'_1 &\leq \frac{m_1}{m_1 + m_2}v_1. \end{aligned} \quad (5)$$

The energy conservation of the bistable mechanism after impact, by adding the kinetic and potential energy, can be written as

$$\frac{1}{2}m_2v_2(t)^2 + \frac{1}{2}k_2x_2(t)^2 = 0. \quad (6)$$

From (4) and (6), the maximum displacement  $\delta_2^{\max}$ , of  $m_2$  can be derived as

$$\delta_2^{\max} = \sqrt{\frac{m_2}{k_2}}v_2 = \sqrt{\frac{m_2}{k_2}}\frac{m_1}{m_2}(v_1 - v'_1) = \frac{m_1}{\sqrt{k_2m_2}}(v_1 - v'_1) \quad (7)$$

$\delta_2^{\max}$  should be larger than the critical displacement,  $\delta_{switch}$ . The value of  $\delta_{switch}$  is determined by the minimum displacement of the bistable mechanism required to switch between its two modes as shown in (Fig. 6(b)). Then

$$\begin{aligned} \frac{m_1}{\sqrt{k_2m_2}}(v_1 - v'_1) &> \delta_{switch} \\ \therefore (v_1 - v'_1) &> \frac{\sqrt{k_2m_2}}{m_1}\delta_{switch}. \end{aligned} \quad (8)$$

The range of values of  $v_1$  for which the bistable mechanism will change states due to an impact force, is referred to as critical velocity,  $v_{1c}$ . The upper limit of  $v'_1$  is reached when both the bistable mechanism and the actuator are moving at the same velocity after contact. Thus, from (5)

$$v'_1 = \frac{m_1}{m_1 + m_2}v_1. \quad (9)$$

Substituting (9) into (8), we can obtain

$$\begin{aligned} \left(v_{1c}^{\text{upper}} - \frac{m_1}{m_1 + m_2}v_{1c}^{\text{upper}}\right) &= \frac{\sqrt{k_2m_2}}{m_1}\delta_{switch} \\ \therefore v_{1c}^{\text{upper}} &= \frac{m_1 + m_2}{m_1}\sqrt{\frac{k_2}{m_2}}\delta_{switch}. \end{aligned} \quad (10)$$

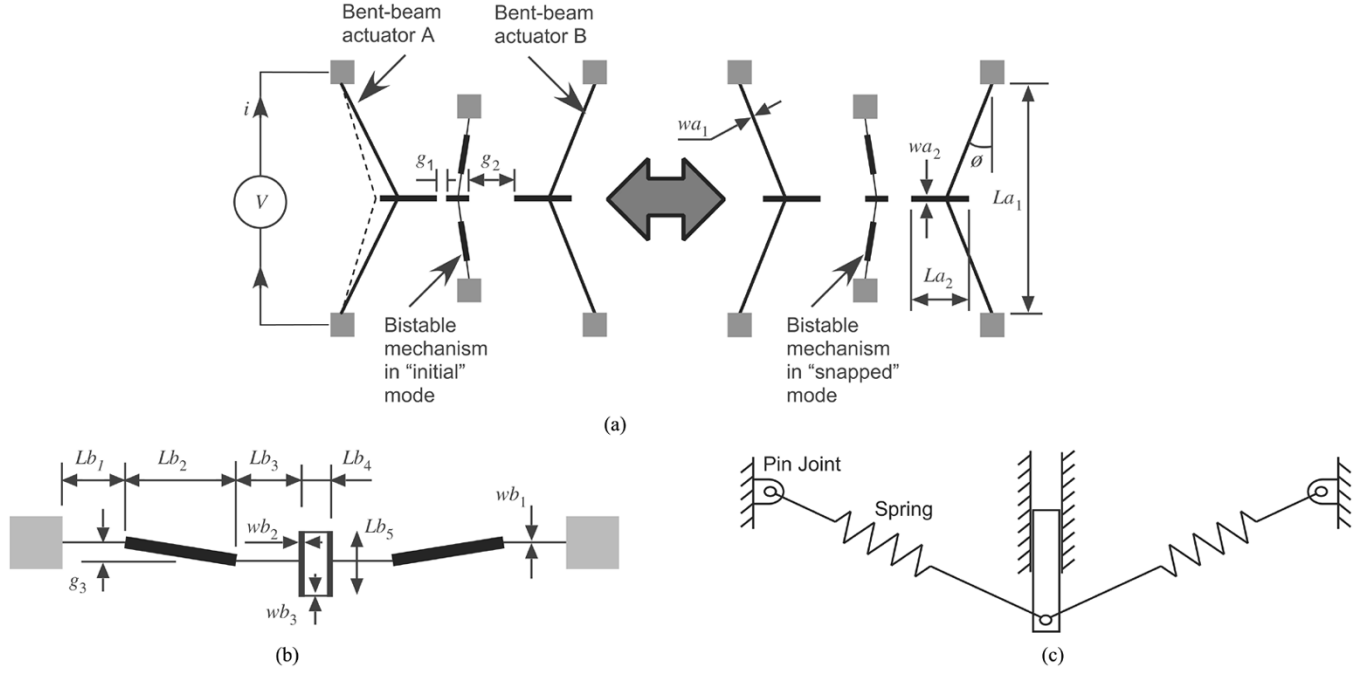


Fig. 7. (a) Schematic of the test structure used to compare pulsed actuation methods, showing bistable mechanism with bent-beam actuators on either side. (b) Bistable mechanism shown with its various elements labeled. (c) Equivalent of the bistable mechanism using pin joints, rods and springs.

The lower limit occurs when the velocity of the actuator drops to zero after contact  $v_1' = 0$ .

Equation (8) then reduces to

$$v_{1c}^{\text{lower}} = \frac{\sqrt{k_2 m_2}}{m_1} \delta_{\text{switch}}. \quad (11)$$

Thus the range for the critical velocity is

$$\frac{\sqrt{k_2 m_2}}{m_1} \delta_{\text{switch}} < v_{1c} < \frac{(m_1 + m_2)}{m_1} \sqrt{\frac{k_2}{m_2}} \delta_{\text{switch}}. \quad (12)$$

Besides the velocity requirement, there is a displacement requirement as well. The tip of the driving engine should make contact with a bistable mechanism for switching to occur. Thus, the displacement requirement is

$$\max(\delta)|_{\text{impact}} = \alpha \delta_{\text{gap}}, \text{ where } (\alpha \geq 1, \alpha \approx 1) \quad (13)$$

where  $\delta_{\text{gap}}$  is the nominal separation between the actuator tip and the bistable mechanism.

If the velocity of the tip is substantially smaller than the critical velocity, but the actuator is driven to sufficient displacement, the switching can be modeled as quasistatic. In order to achieve switching at such low velocities, the tip displacement should exceed  $\delta_{\text{gap}} + \delta_{\text{switch}}$  under the reaction force from the bistable mechanism. Thus

$$\max(\delta)|_{\text{quasi-static}} \approx \delta_{\text{gap}} + \delta_{\text{switch}}. \quad (14)$$

From the viewpoint of energy efficiency, a switching method that requires less energy is preferred, and thus a design that uses impact force may provide improvements in energy efficiency, as a given actuator requires a lesser amount of displacement as indicated by (13) and (14).

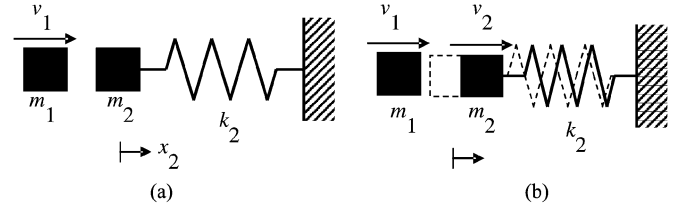


Fig. 8. In order to analyze force generated by bent-beam actuator, the actuator and bistable mechanism are modeled as discrete masses and springs.

### B. Test Structure Design

In order to investigate the influence of impact, two versions of the test structure shown in Fig. 7 were fabricated, Version I and Version II. The dimensions of structures, lower limit of the critical velocities and simulated values of the actuator velocities for different activation methods are shown in Table II. Besides having different bistable mechanisms and actuators, the important difference in the structures lies in the incorporation of an additional mass in Version II with dimensions of  $La_2$  and  $wa_2$ . The additional mass reduces the lower limit of the critical velocity as indicated by (12). The higher velocities attained with burst activation suggests that Version II might generate sufficient impact forces to cause energy savings.

## IV. FABRICATION

Devices were fabricated from 27  $\mu\text{m}$  thick Cu electroplated with SU-8™ as a mold on a Pyrex™ glass substrate, using the process flow shown in Fig. 9. The process starts with evaporating a 3- $\mu\text{m}$ -thick sacrificial layer of Ti. This is followed by sputtering 500 Å thick layers of Ti/Cu/Ti/Si. The Ti is for adhesion, Cu is the seed layer for electroplating and Si is for adhesion of SU-8™. Sputtering is followed by SU-8 lithography

TABLE II  
DIMENSION OF ACTUATORS AND BISTABLE MECHANISM

Parameter	Value (m/s, $\mu\text{m}$ )		Parameter	Value ( $\mu\text{m}$ )	
	Version I	Version II		Version I	Version II
$v_{1c}$	0.6	0.14	$Lb_1$	30	150
$v_l$ - single pulse	0.01	0.01	$Lb_2$	120	550
$v_l$ - burst pulse	0.1	0.1	$Lb_3$	25	150
$La_1$	2000	3000	$Lb_4$	46	25
$La_2$		700	$Lb_5$	100	130
$wa_1$	10	10	$wb_1$	3	3
$wa_2$		20	$wb_2$	18	5
$g_1$	5	5	$wb_3$	10	5
$g_2$	22	60	$\emptyset$ (degrees)	3	3
$g_3$	10	30			

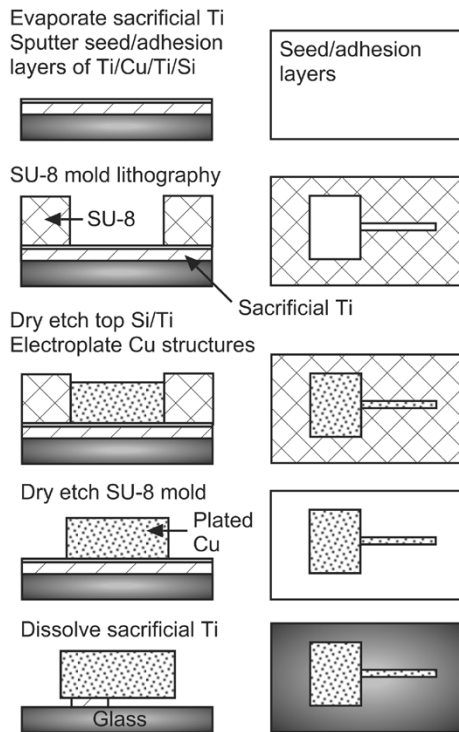


Fig. 9. Single mask UV-LIGA process used to make the test structure. The structural material is electroplated copper.

to make a  $30\text{-}\mu\text{m}$ -thick mold with  $3\text{-}\mu\text{m}$ -wide trenches. The top Ti/Si layers are etched away in a  $\text{CF}_4/\text{O}_2$  plasma to expose the underlying seed layer of Cu. The wafer is then electroplated in a bath with agitation to form the copper structures with an aspect ratio of 10:1. The SU-8 mold is stripped in a  $\text{CF}_4/\text{O}_2$  plasma at high power and the remaining seed layer is etched away in  $\text{HNO}_3$  acid. The structures are released by performing a timed etch on the Ti sacrificial layer in 1:100 HF.

The devices are suitable for unpackaged operation in a laboratory ambient despite the use of Cu, which tends to tarnish. For commercial applications, a thin film of Au or packaging in an inert gas environment may be used. Fig. 10 shows an optical micrograph of Version II of the fabricated test structure. Version I is shown later in Fig. 13.

## V. SIMULATION RESULTS

In order to obtain an understanding of experimental observations, a finite element model of the actuator is developed for the designs that were fabricated. A transient analysis is performed using FEA by ANSYS<sup>TM</sup> to investigate the energy efficiency of actuators. The element type used is SOLID5, which is a coupling solid element that can handle thermal and mechanical fields simultaneously. Joule heating is transformed into an equivalent internal heat generation and heat loss through the air is captured using an equivalent heat transfer coefficient. The dominant mode of heat loss is due to conduction through the air to the substrate, in addition to which, heat dissipation by conduction through the anchors is modeled. The temperature of anchors and ambient environment is assumed to be constant. Material properties used in the analysis are summarized in Table III. The electrical resistivity is determined from the actual resistance of the bent-beam actuators, which is measured to be about  $0.6\ \Omega$ , while the heat transfer coefficient is extracted from experimental results of steady-state actuator tip displacement.

Fig. 11 shows the simulated values of energy and current required for Version II. The simulation indicates that energy consumption reduces at shorter pulse widths, while requiring higher current levels. Also, the energy required can be significantly reduced by assuming that impact switching occurs with burst activation.

## VI. EXPERIMENTAL RESULTS

### A. Electrical Measurements

In order to measure the electrical characteristics of the actuators being testing, the circuit shown in Fig. 12 is utilized. Pulsed actuation is delivered by switching the current  $i$ , through the actuator, using a darlington-pair.  $V_{\text{signal}}$ , generated by a function generator, controls the power transistor. Changing the dc supply voltage  $V_s$  controls actuator power. The voltage across the actuator is measured using a four-point probe method, amplified  $10\times$  by a differential amplifier stage. The actuator current is determined by measuring the voltage drop across a shunt resistor ( $R_{\text{shunt}}$ ), connected in series with the circuit. The amplifiers serve to expand the range of the available instrumentation.

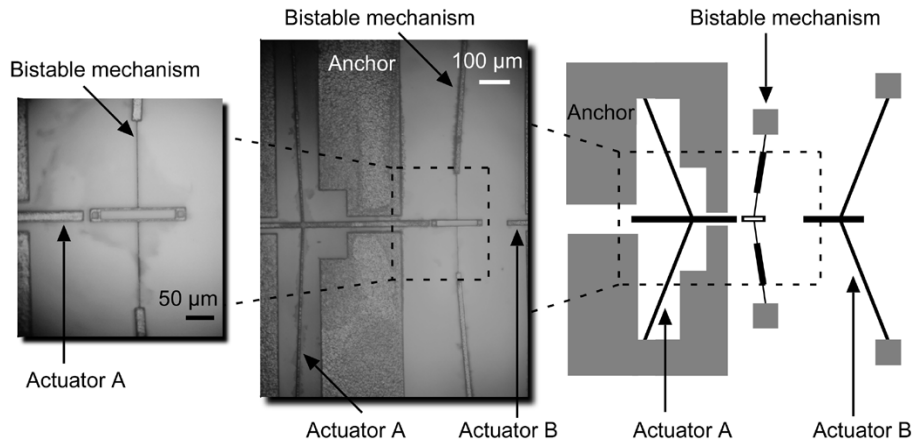


Fig. 10. Optical micrograph of Version II of the test structure, showing Actuator A, the tip of Actuator B and a close up of the bistable mechanism. The actuators have additional masses to enable them to generate appreciable impact forces.

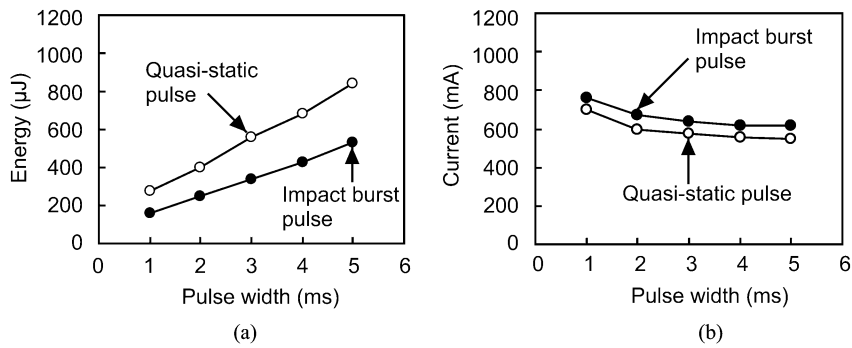


Fig. 11. Simulated values of energy consumed (a) and current (b) through the actuator to switch the bistable mechanism at different pulse widths.

TABLE III  
PARAMETERS OF COPPER USED FOR FINITE ELEMENT SIMULATION

Parameter	Symbol	Value	Units
Young's modulus	$E$	11	GPa
Poisson's ratio		0.33	
Thermal expansion coefficient		$16.8 \times 10^{-6}$	/K
Specific heat	$c_p$	386	J/kg/K
Density	$\rho$	89000	kgf/m <sup>3</sup>
Heat transfer coefficient	$H$	60000	W/m <sup>2</sup> /K
Electrical resistivity		$5 \times 10^8$	$\Omega$ -m

B. Capture of Bistable Modes

In order to determine that an actuator has overcome the set force limit, a change of mode of a bistable mechanism must be observed. The sudden change of mode from initial to snapped is observed from optical micrographs, shown in Fig. 13. A force is applied on the bistable mechanism in the initial mode by pulse driven actuator A. While the force generated by the actuator is less than that of the upper bifurcation point, the bistable mechanism remains in its initial mode. However, if the force applied is greater than that of the upper bifurcation point, a change in mode occurs to the snapped mode. The snapped position when compared to a skeleton of the initial mode can be clearly distinguished.

C. Verification of Reference Force

In order to verify that the bistable mechanism truly provides a fixed reference force, the energy used by an electrothermal actuator to repeatedly snap the structure between its two modes is recorded. Measurements were taken from various devices and arranged into independent data sets. The energy used to switch such a device is shown in Fig. 14. It can be seen the bistable device is switched to the snapped mode repeatedly with a 5 ms pulse at a power of about 100 mW and back to the initial mode at 70 mW. The lower energy required to switch off can be attributed to the unequal energy valleys of the bistable

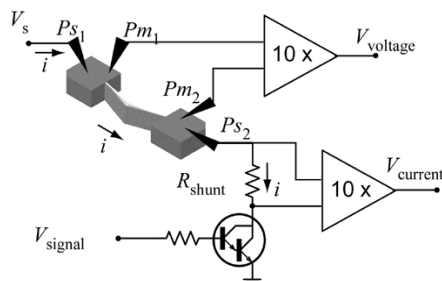


Fig. 12. Schematic of circuit used for pulsed activation and measurement of electrical parameters.

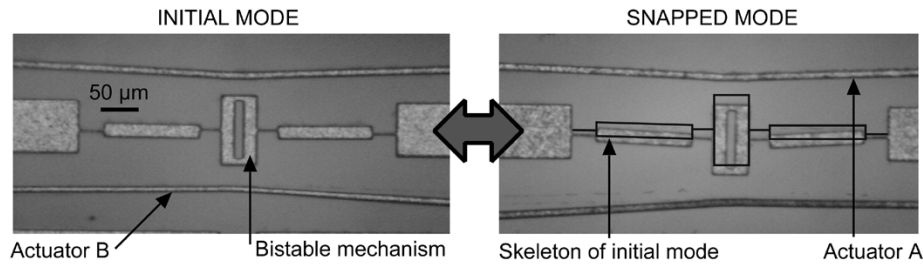


Fig. 13. Optical micrographs of Version I showing the bistable mechanism in the initial mode and the snapped mode.

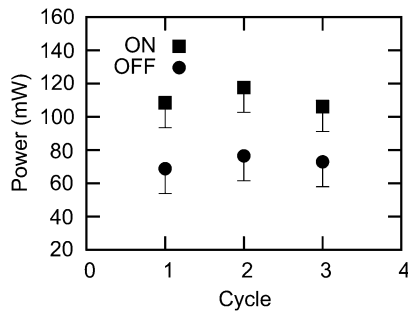


Fig. 14. Using the bistable mechanism repeatedly for a number of cycles provides experimental validation of using the bistable mechanism to generate a reference force.

mechanism. This experimental observation ratifies the use of the bistable structure to provide a minimum loading force.

#### D. Comparison of Pulsed Actuation

In order to compare various pulsed actuation methods, the voltage applied to either actuator A or B is ramped up in 0.1 V steps at a given pulse width until a change in state of the bistable mechanism is observed. This procedure is repeated for different pulse widths. The experiments revealed that it is only possible to cause a change in mode with either actuator A or B using pulsed activation. When powered by a dc voltage the actuator beams fractured at high power levels, and could not generate a sufficient force to effect a mode change in the bistable mechanism. This observation in itself validates the superiority of pulsed actuation, and allows a given actuator to be used more efficiently and generate larger forces.

Fig. 15(a) shows the energy required to change the mode of the bistable mechanism using actuator A and B for Version I. Higher energy efficiency is achieved through the use of short pulses, but comes at the cost of requiring higher current levels as shown in Fig. 15(b). The results follow the same trend when either actuator A or B is used to change the state of the bistable mechanism. The energy consumed using burst actuation is also shown and indicates that no detectable gains in energy efficiency are obtained using the burst mode for Version I, due to only a minor influence of the impact force. The observation is in line with expectations, given the calculated values of critical velocity in Table II. However, the energy efficiency using Version II, shown in Fig. 15(c), is significantly improved using burst actuation. Burst pulses were constructed with trains of pulses of 0.1 ms widths, repeated at 0.2 ms intervals for the duration given by the pulse width. This improved efficiency can be attributed

to the higher velocities attained through pulsed actuation, and the presence of the impact mass.

While a number of process parameters can affect the performance of bistable devices [21], the trends presented in this section were consistent in power, energy and current levels for a large variety of devices.

## VII. CONCLUSION

A theoretical and experimental investigation into the mechanism and benefits of pulse driven bent-beam electrothermal actuators was carried out. A heat transfer analysis revealed that the temperature profile in transient state is more uniform along the length of the beam than that of steady state. Thus, a high input power for a short period results in the same displacement or force while the required energy, which is the product of instantaneous power and the period, is less.

A test structure was designed to compare different activation mechanisms, and made using UV-LIGA electroplated copper structures. The experiment required actuators to overcome a fixed reaction force, as a performance metric, provided by a bistable mechanism. The results showed that it is possible to generate the prescribed amount of force only using pulsed activation methods, and dc activation failed to meet the force requirement. This verifies the superiority of pulsed activation over dc activation, as a method to generate larger forces and displacements with a given electrothermal actuator. Also, moving to shorter activation pulses, results in energy savings of over 80%, which is important for electrothermal actuators that routinely require up to 0.5 W of dc power.

In addition to a thermal model, the dynamics of the generated force were analytically investigated. The analysis defined a critical velocity at which the actuator would generate an appreciable impact force. The value of critical velocity depends on the characteristics of the actuator and the actuated part. To explore the effect of impact on energy consumption, Version II of the test structure was designed. In addition to a structural variation, an alternative burst activation method was developed. Burst activation has the advantage of providing a high velocity at the point of contact, hence increasing the impact force generated. The consumed energy of burst pulse drive was about 70% of single pulse drive if impact switching was achieved. This reveals that the burst pulse drive could achieve an appreciable impact force, which was not seen with a single pulse drive. An energy savings with burst drive could only be achieved using Version II, which highlights the importance of a well-tailored design.

Pulsed activation has been shown to be advantageous while using electrothermal actuators, as it can be used to extract a large

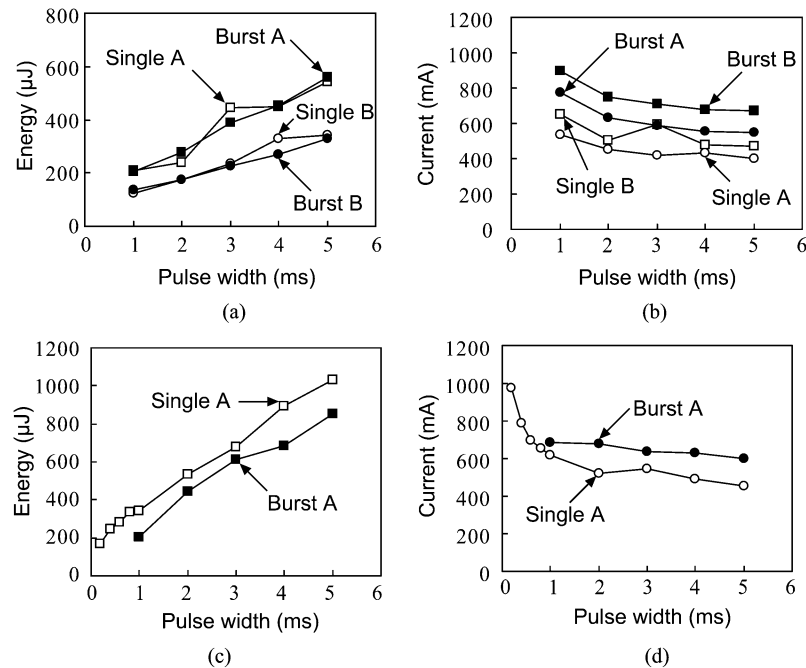


Fig. 15. (a) Version I: the amount of energy required by an actuator to switch the bistable mechanism reduces as activation is carried out with shorter pulses. Also, the use of burst pulses shows no appreciable change in the energy requirement. (b) The use of shorter pulse results in higher values of instantaneous current through the actuator. (c) and (d) Version II: the same trend in energy and current requirement is observed as that for Version I when using single pulses. However, the use of burst activation results in a reduction of the required energy, which is not achievable for Version I.

amount of force and displacement with a given actuator. Further investigations may be carried out to optimize the structure of the actuator in order to achieve a uniform temperature profile and optimize its dimensions accordingly.

## REFERENCES

- [1] J. Que, J.-S. Park, and Y. B. Gianchandani, "Bent-beam electrothermal actuators—Part II: Linear and rotary microengines," *J. Microelectromech. Syst.*, vol. 10, pp. 255–262, Jun. 2001.
- [2] J. M. Maloney, D. S. Schreiber, and D. L. DeVoe, "Large-force electrothermal linear micromotors," *J. Micromech. Microeng.*, vol. 14, no. 2, pp. 226–234, Feb. 2004.
- [3] C. Lee, Y.-S. Lin, Y.-J. Lai, M. H. Tasi, C. Chen, and C.-Y. Wu, "3-V driven pop-up micromirror for reflecting light toward out-of-plane direction for VOA applications," *IEEE Photonics Technology Letters*, vol. 16, Apr. 2004.
- [4] J. C. Chiou and W. T. Lin, "Variable optical attenuator using a thermal actuator array with dual shutters," *Opt. Commun.*, vol. 237, no. 4-6, pp. 341–350, Jul. 2004.
- [5] K. Udeshi and Y. B. Gianchandani, "A DC-powered, tunable, fully mechanical oscillator using in-plane electrothermal actuation," *Proc. IEEE Micro Electro Mechanical Systems (MEMS)*, pp. 502–505, 2004.
- [6] —, "A transistorless micromechanical high voltage generator using a DC-powered self-oscillating relay," in *Proc. Solid-State Sensor, Actuator and Microsystems Workshop*, 2004, pp. 262–265.
- [7] L. Que, K. Udeshi, J. Park, and Y. B. Gianchandani, "A bistable electro-thermal RF switch for high power applications," *Proc. IEEE Micro Electro Mechanical Systems (MEMS)*, pp. 797–800, 2004.
- [8] Y. Wang, Z. Li, D. T. McCormick, and N. C. Tien, "A low-voltage lateral MEMS switch with high RF performance," *J. Microelectromech. Syst.*, vol. 13, Dec. 2004.
- [9] E. T. Enikov and K. V. Lazarov, "Composite thermal micro-actuator array for tactile displays," *Proc. SPIE, Smart Structures and Materials: Smart Electronics, MEMS, BioMEMS, and Nanotechnology*, vol. 5055, pp. 258–267, Mar. 2003.
- [10] L. Que, J.-S. Park, and Y. B. Gianchandani, "Bent-beam electrothermal actuators for high force applications," *Proc. IEEE Micro Electro Mechanical Systems (MEMS)*, pp. 32–35, 1999.
- [11] —, "Bent-beam electrothermal actuators—Part I: Single beam and cascaded devices," *J. Microelectromech. Syst.*, vol. 10, pp. 247–254, 2001.
- [12] C. D. Lott, T. W. McLain, J. N. Harb, and L. L. Howell, "Modeling the thermal behavior of a surface-micromachined linear-displacement thermomechanical microactuator," *Sens. Actuators A, Phys.*, vol. 101, pp. 239–250, 2002.
- [13] A. Geisberger, N. Sarkar, M. Ellis, and G. Skidmore, "Electrothermal properties and modeling of polysilicon micro thermal actuators," *J. Microelectromech. Syst.*, vol. 12, pp. 513–523, Aug. 2003.
- [14] L. Que, L. Otradovec, A. D. Oliver, and Y. B. Gianchandani, "Pulse and DC operation lifetimes of bent-beam electrothermal actuators," *Proc. IEEE Micro Electro Mechanical Systems (MEMS)*, pp. 570–573, 2001.
- [15] M. Taher and A. Saif, "On a tunable bistable MEMS—Theory and experiments," *J. Microelectromech. Syst.*, vol. 9, pp. 157–170, Jun. 2000.
- [16] B. D. Jensen, M. B. Parkinson, K. Kurabayashi, L. L. Howell, and M. S. Baker, "Design optimization of a fully-compliant bistable micro-mechanism," in *Proc. 2001 ASME Int. Mech. Eng. Congress and Exposition*, pp. 1–7.
- [17] J. Qiu, J. H. Lang, and A. H. Slocum, "A curved-beam bistable mechanism," *J. Microelectromech. Syst.*, vol. 13, Apr. 2004.
- [18] J. M. Maloney, D. S. Schreiber, and D. L. DeVoe, "Analysis and design of electrothermal actuators fabricated from single crystal silicon," in *Proc. 2000 ASME Int. Mech. Eng. Congress and Exposition, MEMS*, vol. 2, pp. 223–239.
- [19] L. Lin and M. Chiao, "Electrothermal responses of lineshape microstructures," *Sens. Actuators A, Phys.*, vol. 55, pp. 35–41, 1996.
- [20] L. Meirovitch, *Fundamentals of Vibration*. New York: McGraw-Hill.
- [21] J. W. Wittwer, L. L. Howell, S. M. Wait, and M. S. Chery, "Predicting the performance of a bistable micro mechanism using design-stage uncertainty analysis," in *Proc. 2002 ASME Int. Mech. Eng. Congress and Exposition, IMECE2002-33 262*, pp. 127–134.



**Yoshinobu Shimamura** received the B.S., M.S., and Dr.Eng. degrees in mechanical engineering from Tokyo Institute of Technology, Japan, in 1993, 1994, and 2000, respectively.

From 1994 to 2005, he was an Assistant Professor at the Tokyo Institute of Technology. Since 2005, he has been an Associate Professor in the Department of Mechanical Engineering at the Shizuoka University. From 2003 to 2004, he was a Visiting Scholar at the University of Michigan, Ann Arbor, for the research on the mechanics and applications of electrothermal

bent-beam actuators. His current research interests include fracture and durability of metal and composite materials.



**Kabir Udeshi** was born in India in 1978. He received the B.E. degree in mechanical engineering from The University of Pune in 2000 and the M.S. degree from the University of Michigan, Ann Arbor, in 2003. He is currently pursuing the Ph.D. degree in mechanical engineering while focusing on the development of micromachined fully mechanical oscillators and their applications.

During his undergraduate career, he interned at Larson & Toubro Ltd. and Tata R&D Laboratories. His work included the design and manufacturing of a prototype tape dispenser and the design and testing of a thermo-electric cooling system to be used in an armored vehicle. His initial work as a Graduate Student was toward the manufacturing setup and assembly of muon particle detectors used for the ATLAS experiment at CERN, Switzerland. His other interests include RF switches, optical pulse shaping on a chip and applications of microelectrodischarge machining. He has been a reviewer for *JMEMS* and *Sensors and Actuators*.



**Long Que** (M'00) received the undergraduate and graduate education degrees in physics and communication from Peking University, Beijing, China. He received the Ph.D. degree in electrical engineering from the University of Wisconsin-Madison in 2000.

Presently, he is with GE Global Research. Prior to this, he worked at the Center for Nanoscale Materials at Argonne National Laboratory, Argonne, IL, focusing on nanoscience and nanotechnology. He was a Visiting Research Scientist and Research Fellow at the Electrical Engineering and Computer Science (EECS) Department and the Center for Wireless Integrated Microsystems (WIMS) of the University of Michigan, Ann Arbor. His research interests are in bioMEMS/optical/RF/nano MEMS, nanoscience and nanotechnology. He has published one book chapter in MOEMS, more than 20 papers in journals and conferences, has been awarded four U.S. patents, and has 10 patents pending.

Dr. Que won a National Research Award from the Chinese Academy of Sciences in 1997 and the Vilas Professional Development Fellowship from University of Wisconsin in 2000. He is a Member of SPIE.



**Jaehyun Park** received the B.S. and M.S. degree in precision mechanical engineering from Hanyang University, Seoul, Korea, in 1998 and 2000, respectively. He is currently pursuing the Ph.D. degree at the Electrical Engineering and Computer Science Department at the University of Michigan, Ann Arbor.

His research interests include fabrication of MEMS structures and microsystems for cell culture and biology.



**Yogesh B. Gianchandani** (S'83-M'85-SM'04) received the B.S., M.S., and after some time in industry, the Ph.D. degree in electrical engineering, with a focus on microelectronics and MEMS.

He is presently an Associate Professor in the EECS Department and holds a joint appointment in the Department of Mechanical Engineering at the University of Michigan, Ann Arbor. Prior to this, he was with the ECE Department at the University of Wisconsin, Madison. He has also held industry positions with Xerox Corporation, Microchip Technology, and other companies, working in the area of integrated circuit design. His research interests include all aspects of design, fabrication, and packaging of micromachined sensors and actuators and their interface circuits. At the University of Michigan, he serves as the Director of the College of Engineering Interdisciplinary Professional Degree Program in Integrated Microsystems.

Prof. Gianchandani is the recipient of a National Science Foundation Career Award, and he has published about 150 papers in the field of MEMS, and has about 25 patents issued or pending. He serves on the editorial boards of *Sensors and Actuators*, *IOP Journal of Micromechanics and Microengineering*, and *Journal of Semiconductor Technology and Science*. He also served on the steering and technical program committees for the IEEE/ASME International Conference on Micro Electro Mechanical Systems (MEMS) for many years, and served as a General Co-Chair for this meeting in 2002.